https://doi.org/10.3311/PPci.24006
Creative Commons Attribution

Periodica Polytechnica Civil Engineering, 70(1), pp. 133–150, 2026

Evaluation of the Two Faces Water Level Dynamics and its Impact on the Stability of Railway Embankment Infrastructures

Bamaiyi Usman Aliyu[1,3*], Xu Linrong[1,2], Al-Amin Danladi Bello[3], Li Yongwei[1,2], Abdulaziz Ahmad[1,4], Li Shengxiang[1,2]

[1] Department of Geotechnical Engineering, School of Civil Engineering, Central South University, No. 172 Tongzipo Road, 410075 Changsha, Hunan, China
[2] National Engineering Laboratory for High-Speed Railway Construction, School of Civil Engineering, Central South University, No. 172 Tongzipo Road, 410075 Changsha, Hunan, China
[3] Department of Water Resources & Environmental Engineering, Faculty of Engineering, Ahmadu Bello University, P. M. B. 1045, 810106 Zaria, Nigeria
[4] Department of Civil Engineering, Faculty of Engineering, Ahmadu Bello University, P. M. B. 1045, 810106 Zaria, Nigeria
* Corresponding author, e-mail: usmanaliyu@abu.edu.ng

Received: 03 December 2023, Accepted: 05 January 2026, Published online: 09 February 2026

Abstract

The Nanhu railway embankment, located between two lakes, experiences seasonal water level fluctuations. This study aims to assess the impacts of these fluctuations on embankment seepage, stability, and deformation conditions. Firstly, field observations and laboratory experiments were conducted to determine the hydro-mechanical properties of the embankment material and the drawdown scenarios. Subsequently, GeoStudio 2D and PLAXIS 2D software were used for numerical analysis. The analysis demonstrates that the combined impact of a train static load (130–150 kPa) with lowering drawdown and increasing water level scenarios affects the stability of the embankment, resulting in more deformation than the falling scenario. The model result showed a maximum displacement of 238.43 mm, which was corroborated by the observed field data. Furthermore, the rising scenario had a minimal safety factor of 0.9128, and the falling scenario yielded a minimum safety factor of 0.9312, indicating severe instability. Furthermore, the findings indicate that understanding the relationship between safety factors, pore-water pressure, deformation, and train static load for an embankment infrastructure can aid in the stability management of multi-face water level fluctuation conditions. To prevent embankment failures, simplified preventive approaches are analyzed, and it is discovered that the steel-pipe grouting consolidation method can potentially enhance embankment stability by 50%.

Keywords

slope stability, pore pressure-strain coupling, deformation, lake water level, safety factor, steel pipe grouting reinforcement

1 Introduction

The presence of railway infrastructure plays a crucial role in facilitating transportation, fostering economic development, and ensuring the availability of a reliable and secure mode of transit for both passengers and goods [1]. These infrastructures are often exposed to natural geo-hazards, such as floods [2], rainfall, earthquake, water ponding, landslides [3], and other similar events. These hazards have the potential to compromise the stability and performance of these infrastructures. Water-related hazards, such as rainfall, ponding, and fluctuating water levels, have the potential to induce soil erosion, mass movement, slope instability, and embankment collapse. The occurrence of transportation embankment failures not only hinders railway operations but also presents a significant risk to public safety and the environment [4]. The future is expected to witness an increase in heavy rainfall as a consequence of climate change [5]. Consequently, it is important to investigate the effects of water level fluctuations resulting from different rainfall events on the stability of the transit embankment. Various factors, including seepage, erosion, slope characteristics, load distribution, cracks, aging, rainfall patterns, environmental variability, and soil quality, can collectively influence the effects of water level fluctuations. Multiple studies have indicated that

Cite this article as: Aliyu, B. U., Linrong, X., Danladi Bello, A.-A., Yongwei, L., Ahmad, A., Shengxiang, L. "Evaluation of the Two Faces Water Level Dynamics and its Impact on the Stability of Railway Embankment Infrastructures", Periodica Polytechnica Civil Engineering, 70(1), pp. 133–150, 2026. https://doi.org/10.3311/PPci.24006

railway networks are susceptible to water-related issues, which are driven by a combination of topographical and climatic elements [6].

On November 1, 2020, an incident took place in China where a subsidence of 6 mm caused deformation in the rail-bed slope. Subsequently, after four days, the deformation of the roadbed slope worsened, resulting in extensive deformation and landslides on the subgrade slope. Consequently, the affected area became blocked. On the aforementioned day, the settlement amount reached a total of 232 million, and a vertical displacement of over 1.2 m. Subsequently, measures were implemented to enhance the management of the issue. The act of inserting concrete piles into the side of the preexisting embankment was performed, although it was subsequently determined that this method of driving the piles into the sliding surface did not effectively resolve the issue at hand. This phenomenon led to an escalation in mass and subsequently exacerbated subsidence, leading to the breakdown of the embankment. Consequently, the frequent instances of embankment failure highlight the importance of effectively monitoring and managing deformations in roadbed slopes, landslides, and train-induced vibrations. The assessment of these components is of utmost importance in order to achieve slope stability and mitigate potential future harm.

The present study investigates the impact of water fluctuation on the railway embankment in Yueyang region, China. The Nanhu Railway Embankment (NRE) serves as a barrier between two lakes that experience fluctuating water levels as a result of seasonal rainfall patterns influenced by climate change. Over the course of several years, there have been numerous instances of railway embankment failures, leading to significant interruptions in train operations and requiring expensive restoration efforts. Understanding the behavior of embankment structures under varying water levels on both sides is crucial. Previous research has primarily focused on examining the change in water levels in a single face [7]. The key factor contributing to embankment failure during the water drawdown process is the variation in water levels, whether they are decreasing or increasing. Therefore, it is imperative to evaluate the stability of the NRE in light of fluctuations in water levels along the embankment surfaces.

Several methods have been developed to evaluate the impact of water fluctuation on the stability of the embankment structure. Nevertheless, certain techniques, such as computational fluid dynamics, discrete element approaches, and deformation analysis methods, exhibit various levels of uncertainty [8]. The present investigation employed finite element method (FEM) analysis due to its recognized effectiveness, particularly when the modeling parameters are accessible [9]. This approach proves particularly advantageous when the properties of the embankment soil, including cohesion, friction angle, and other hydro-mechanical characteristics, are known. Burman et al. [10] assert that the Finite Element Method (FEM) is a dependable approach for assessing the slope stability of an embankment under conditions of continuous water level fluctuation. The utilization of this method is suitable for intricate environments such as the NRE scenario due to its ability to yield crucial analytical information, including the spatial distribution of pore water pressure, the redistribution of stress, and the patterns of displacement. These parameters are challenging to identify through alternative approaches [11]. Numerous computer-based numerical simulation techniques have been developed for the purpose of enhancing the assessment of geotechnical challenges, since they have demonstrated efficacy in resolving diverse geotechnical concerns. This study used the Finite Element Method (FEM) to analyze the stability of an embankment under different saturation circumstances. The findings indicate that the interaction between drawdown in the reservoir and intense rainfall events has a destabilizing effect on the embankment, leading to landslides. A previous study [9] using the Finite Element Method (FEM) in the PLAXIS model showed that when the length or intensity of rain increases, so do surface deformation, excess pore water pressure, and stress. Additionally, it was also noted that there is a decrease in matric suction under these circumstances [12]. In the study conducted by Gu et al. [13], it was observed that hydraulic hysteresis occurs along the saturation line of the embankment slope. The fluctuation of water levels under these conditions poses a risk to the stability of the structure. Furthermore, a comparison of the results obtained from the two models employed in the study indicates that the deterministic model tends to overlook the spatial variability of soil strength parameters. Additionally, this suggests that there will be an increase in safety concerns during the process of water rising as well as during the rising-constant-falling phases. In fact, the Finite Element Method (FEM) offers a more comprehensive understanding of the influence of geo-hazards on embankment structures, particularly when multiple models are employed to verify the resulting output [14, 15]. The Nanhu embankment was submerged for two months, from mid-July 2020 to early September 2020. Subsequently, as the lake water receded steadily, there was a vertical displacement of over 1.2 m.

This led to a disruption in train traffic lasting 41 hours, causing an economic loss of 70 million yuan. However, the Nanhu embankment has not been thoroughly investigated to understand the extent of the impacts of the water level fluctuation in the two lakes.

The main objective of this study is to evaluate the impact of water level fluctuations on the two sides of the embankment, considering different soil zones and track loads in an unsaturated state. Consequently, the two Finite Element Method (FEM) software applications, namely PLAXIS 2D [16] and GEOSLOPE (in the package of GeoStudio 2D [17]), are employed. Both software programs utilized the strength reduction approach to calculate the safety factor of the embankment slope. The GEOSLOPE (GeoStudio 2D) technique is commonly referred to as the stress redistribution technique. The aforementioned algorithms have demonstrated enhanced resilience and persuasive capabilities in the investigation of embankment instability concerns [1, 12]. According to the literature, the stress redistribution technique emerges as a more favorable alternative for the evaluation of stability studies [18].

The present paper is organized in the following manner:

- Section 2 provides a concise overview of the framework and methodologies, along with details regarding the data source, hydrological characteristics, site topography, and mechanical and physical properties of the embankment utilized in the investigation.
- Section 3 of the paper delves into an examination of the loading conditions, mechanical and physical characteristics of the embankment, the numerical approaches employed, and the parameters utilized in the research.
- Section 4 provides a comprehensive analysis and evaluation of the obtained results.
- Section 5 serves the purpose of summarizing the investigative findings and deriving the conclusions of the study. The outcomes of this research will provide valuable insights for stakeholders engaged in the planning, design, and maintenance of railway infrastructure, as well as the broader field of geotechnical engineering. Specifically, it will furnish pertinent data regarding the enduring stability of railway embankments when subjected to fluctuating water levels.

2 Materials and methods

2.1 Geological and hydrological conditions of the Nanhu Railway Embankment

The Nanhu Railway Embankment (along Beijing-Guangzhou Railway) is situated in Yueyang City, Hunan province, 113°05′00.46″ E, 29°20′48.66″ N, is characterized by complex geological and hydrological settings. Hydrologically, the area is characterized by a humid subtropical climate, with varied rainfall intensity and high humidity. The region is also affected by monsoon rains, which can lead to flash floods and landslides [19]. The K1430 + 110 section of the Beijing-Guangzhou Railway embankment in Fig. 1 [20] is positioned to the east of South Lake and borders Dongting Lake to the west. Situated in close proximity to the lake shore, the study area features an extensively interconnected river network, contributing to the widespread occurrence of soft soil. Constructed in 1999, the Nanhu railway embankment comprises 16 m of artificial fill, including silty clay and a layer of muddy clay. One side of the embankment is exposed to Dongting Lake, making it vulnerable to the impacts of lake water level fluctuations, which lead to the collapse of a 170 m long section of the embankment during a water level recession. The lake also plays a crucial role in flood control in the region, and its water level fluctuations can significantly impact the stability of the surrounding embankments and slopes. The area is prone to flooding due to its low-lying topography and proximity to large water bodies, including Dongting Lake and the Yangtze River.

In terms of Geology, Dongting Lake, located in the Dongting Basin bounded by mountains, occupies the lowest elevation within the basin. Over the geological ages, from the Cretaceous to the Paleogene, the plain experienced sediment accumulation with a thickness ranging from 3000 to 6000 m [21]. Quaternary period played a pivotal role in influencing the modern lake basins, marked by three different stages of tectonic growth in the Dongting Basin. Initially, during the early to middle Pleistocene, the basin underwent tectonic subsidence. Subsequently, in the late-middle Pleistocene, there was an overall uplift of the Dongting Basin, leading to extensive denudation. The third stage witnessed a renewed sinking of the Dongting Basin from the Holocene onward, a trend that persists to the present day [22]. The Holocene strata contain clay while the Pleistocene strata consist of sand, creating the phreatic aquifer and the confined aquifer, respectively [22].

To understand the basis on which the drawdown scenarios were selected, the annual water level variations and background of Dongting become important, see Fig. 2. The lake's area is typically about 2,820 km^2. Still, yearly between July–September period, flood water flows from the excess Yangtze River into the lake, leading to an increase in area to about 20,000 km^2 in flooding season, when vast amounts of sediment-water flow from the

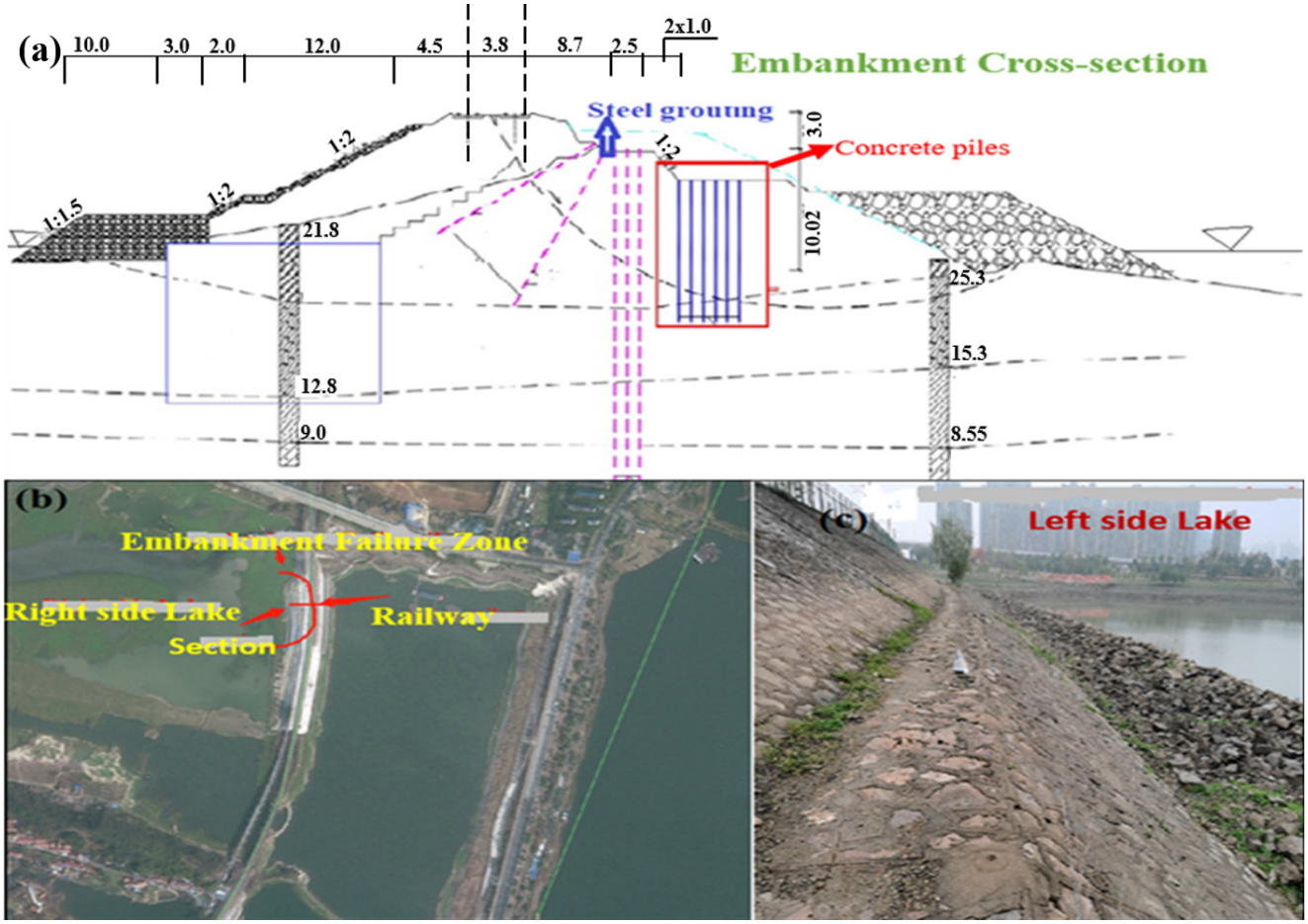

Fig. 1 (a) Cross-section of the embankment, (b) Study area location, and (c) Photo of the left side lake view [20]

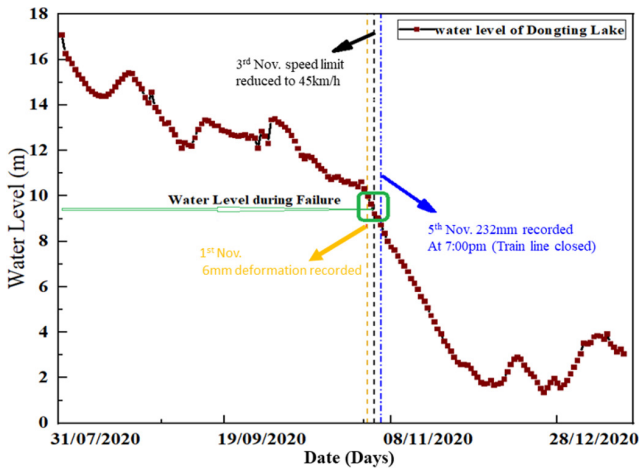

Fig. 2 The annual water level variations at Dongting Lake from 2020-2021

tributaries into the lake. Therefore, the factors contributing to slope instability resulting from changes in lakes water levels are essential for grasping the mechanisms of water seepage in lakes and effectively mitigating and preventing railway embankment failure.

2.2 Model development

Fig. 3 illustrates the procedures and steps of the model development in this study. The data on the soil hydro-mechanical characteristics were obtained via laboratory analysis, as depicted in Table 1, and the data from the storm cycle monitoring system was obtained from the field was collected for the period of 2020 to 2021. These represent the phases of the drawdown pattern used to develop the two scenarios (rising and falling water levels), as shown in Fig. 2. The lake water level fluctuation is acknowledged through this phase to understand the exceedance probability of the event annually.

2.2.1 Numerical model setup

The Nanhu Railway Embankment model was developed by considering section K1430 + 110, which was drawn using the computer-aided design tool (AutoCAD software [23]). Subsequently, it was imported into the numerical software (PLAXIS 2D [16] and GeoStudio 2D [17]) for analysis (see Fig. 3). This involved the creation of a finite element model

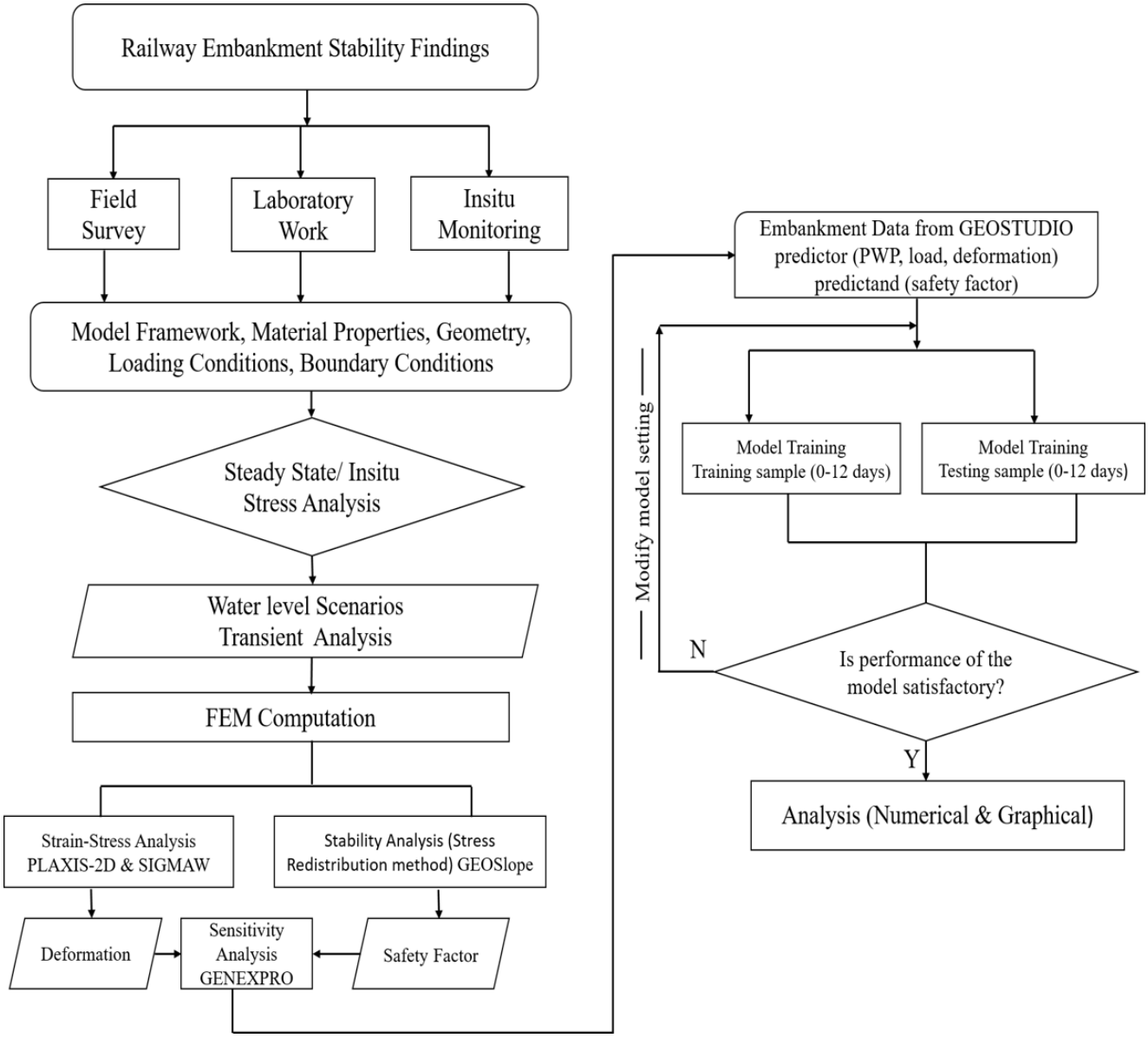

Fig. 3 Study flowchart

Table 1 Nanhu embankment site hydro-mechanics parameters

S/N	Material type	Volumetric weight (KN/m^3)	Cohesion (kPa)	Internal friction angle (°)	Saturated water content (%)	Permeability coefficient (m/s)	Poisson ratio	Elastic modulus (MPa)
1	BST4	19	14	34	30	5.30×10^{-6}	0.30	23.5
2	BST3	20.3	19	34	27.7	4.86×10^{-6}	0.29	26.2
3	BST2	21	21	36	27	3.54×10^{-6}	0.25	38.2
4	BST1	21	22	36	29	2.50×10^{-6}	0.25	38.0

of the embankment section with an unstructured grid size consisting of triangular and quadrilateral elements. The initial steady-state seepage hydraulic boundary condition was set at 53.3 m for both lakes. This height was selected because it is the average depth of the water observed over a period of two years. The model section was divided into four segments because a deep soil investigation of the soil layer over a depth of 75 m shows that varied soil layers exist in the embankment structure. The foundation level is loamy clay, the subgrade is made of clay, the subbase consists of silty clay, and the embankment superstructure is constructed from a composite material (labeled BST1 and BST4, respectively) with an elevation of 13.5 m from the subbase. The coupled water-soil interaction criterion was applied to all soil layers. Two

hydraulic boundary conditions were created and used for the analysis based on monitoring hydrological data at the site for the drawdown scenarios, which was considered appropriate for the change in water level as previous studies confirmed that boundary conditions are site-specific [24]. In this study, the boundary conditions selected based on the study area are water level on both sides of the embankment slope, the rail track loads, the geological conditions of the site, and other environmental conditions (Water level fluctuation, embankment material, and grouting).

2.2.2 Evaluation of the seepage, deformation, and stability of Nanhu Railway Embankment

The seepage, deformation, and stability were modeled and examined using the GeoStudio 2D [17] program with the SEEPW, SIGMAW, and SLOPEW modules, respectively (Fig. 3). In this research, the stability of a submerged roadbed is tested under two different drawdown scenarios using coupled transient-seepage and elasto-plastic soil deformation FEM numerical analysis. The stress and seepage-induced pore pressure conditions and their dissipation criteria are also taken into account. To further check the deformation predicted using GeoStudio 2D [17], the FEM code PLAXIS 2D [16] was employed to validate the model result and its prediction accuracy and further compare it with the observed deformation obtained at the site during failure processes. To evaluate the stress–pore pressure deformation analysis, an FEM mesh with an unstructured global grid size of 1m was used, consisting of 19,345 triangular and quadrilateral elements. The analysis conditions were categorized into two steps. The first step is the initial water level condition of the lakes, which is at 53.5 m. The second step involves the two scenarios described in Section 2.2.1 for both lakes over a period of 20 days during the transient state. Presently, there is no data regarding the surface water interaction/groundwater or lag times for the study area [25]. Therefore, an instantaneous pore water pressure change and the lake level variations were employed to define the model boundary conditions for both falling (0.2 m/day) and rising (0.1 m/day) scenarios used in the FEM analysis. The bottom and side surfaces were fixed during the displacement analysis.

Seepage analysis

The model includes four different soil layers, as mentioned above in Section 2.1. The hydraulic conductivity changes and soil-water characteristics curves (SWCC) for the unsaturated materials are shown in Fig. 4. As summarized in Table 1, the general hydro-mechanical parameters of the four soil structures are evaluated in the laboratory. The initial steady-state seepage line of the embankment from the two sides of the lake was determined from the datum elevation of the water level derived from the data of the monitoring stations at the lake. It is important to note that all two scenarios are simulated in the model with reference to the defined benchmark. The seepage field was simulated using the settings that the volumetric water content (VWC) and permeability coefficient of the two upper layers of the embankment were a function of the pore-water pressure (PWP) of the slope, as stated by Shoaib et al. [26]. The scenarios are evaluated by computing the peak rate of fluctuation of the lake water level with a minimum rate of 0.1 m/day and 0.2 m/day for rising and falling scenarios, respectively. For clarity, the two scenarios are defined as follows:

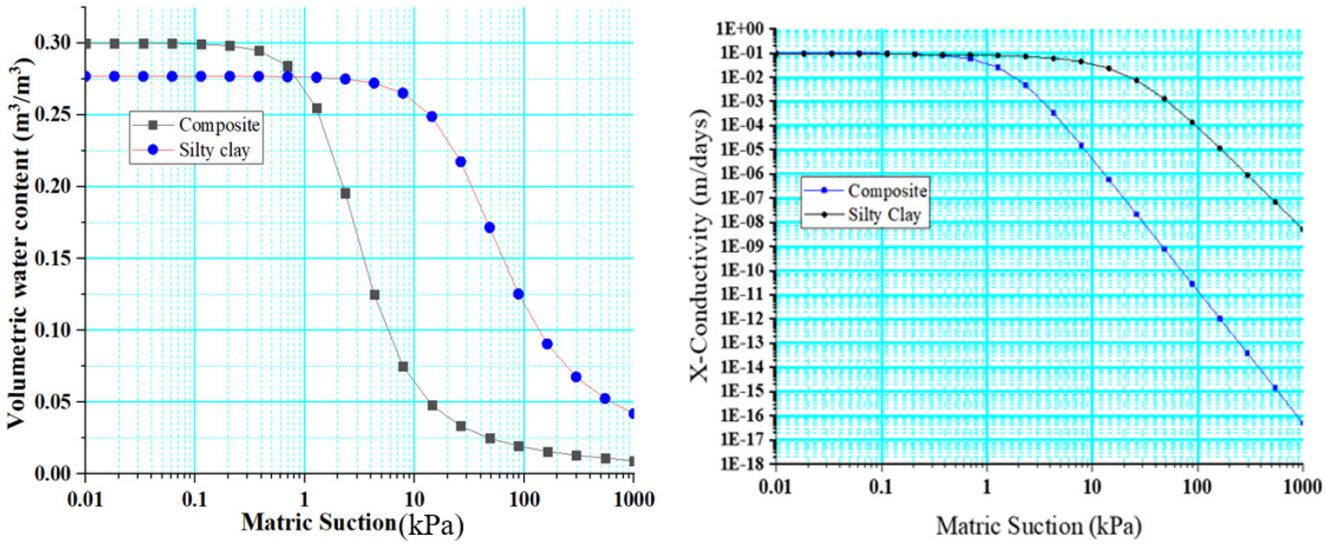

Fig. 4 Hydraulic conductivity and SWCC curves for Nanhu embankment

1. Scenario 1: rising water level, from 53.5 m to 71.2 m and 53.5 m to 58 m;
2. Scenario 2: falling water level, from 71.2 m to 53.5 m and 58 m to 53.5 m.

A review of the historical field data has shown that the critical change in water level in the lake during the summer/autumn season happens within 20 days. Consequently, 20 days were set for the seepage analysis under varied drawdown conditions to compute the stability of the embankment slope. Some previous studies depicted that the most influential change in water level and antecedent precipitation on slope stability begins at 5 days and above [27]. The steady-state boundary conditions were defined using the field data, as illustrated in Fig. 1, in which the minimum water level is referred to as the groundwater in Table 1, and the flux sections were adopted in the seepage model setup to calculate the flow of water in the embankment slope. Both steady-state and transient conditions were analyzed, with steady-state used to check the reasonableness of transient results. The maximum water level of 17.17 m obtained from the observed data was used for the transient analysis.

Loading conditions

The total embankment loadings comprise the embankment deadload, drawdown loadings, and Train system loads. The train system loadings are further divided into three, namely, the ballast load, track system load, and train axle stress, this exact influence on the sliding surface. According to the previous study [25], in situ stresses for a loaded track system range between 45 to 60 kPa.

The ballast load is calculated using the standard value of the bulk density of compacted ballast.

Therefore,

$$\text{Ballast load} = \frac{k_b \times g \times t}{1000} \tag{1}$$

where k_b is bulk density, t is the thickness of ballast, and g is gravity.

The ballast load was determined to be 4.5 kPa. Train axle load for class C4 and D4 (international Union of Railway) is 80 KN/m (worse case). Therefore, the total distributed stresses from the train system used for the analysis is 130–150 kPa.

Deformation process and analysis

The deformation analysis was conducted following the generation of geostatic stress conditions from the seepage analysis using SIGMA/W (in part of the GeoStuido 2D [17]) and PLAXIS 2D [16]. This approach allowed for the inclusion of pore-pressure-induced deformation resulting from changes in loading conditions under time-dependent hydraulic conditions in both unsaturated and saturated soil. The numerical process utilized a modified non-linear elasto-plastic soil model to accurately capture the soil behavior. The behavior of unsaturated soils and the influence of suction above the water in Table 1 can be effectively analyzed using the fully coupled flow-soil deformation approach. In this study, the initial conditions for the modeling process were set, considering both the effects of train track load and slope gravity loading.

Stability analysis

Finite Element Method (FEM) analysis in GEOSLOPE was utilized to evaluate the variations in the external impact of water [28] and train track loads to assess the behavior or condition of the embankment slope using the hydro-mechanical FEM concept. The hydro-mechanical analysis conducted, as shown in Table 1, aims to account for transient flow and differential deformation, subsequently, the stability analysis for the specific time period based on the observed water level (Fig. 2). The stability analysis in this study is designed to estimate the Factor of Safety (FOS) using the advanced principle of stress redistribution technique [11], which differs from the traditional FEM approach of the strength reduction method for determining failure. The study was necessitated due to the subsidence incident of Nanhu embankment, which occurred in China on November 1, 2020, and resulted in roadbed slope deformation. Despite efforts to address the issue, including driving concrete piles, these attempts were unsuccessful, leading to embankment failure. Effective evaluation of the causes of failure that will pave the way for mitigation measures is crucial to prevent the failure, and its management, improve its stability and further prevent future damage. Therefore, the stability analysis is derived from the current observed conditions of the Nanhu embankment as mentioned earlier (see Section 2.2.1) and they are evaluated based on the uniqueness of the embankment two face water level fluctuation.

2.3 Evaluating the relationship between PWP, deformation, static load, and safety factor

In this study, to determine the relationship between deformation, static load, PWP, and safety factor, a data-driven approach (DDA) such as GeneX programming is employed to check the connection and develop a model for these parameters.

GEP (Gene Expression Programming) is a modified genetic algorithm tool for prediction models that tries to mimic the evolution of living biological organisms [29]. It comprises five basic functions: fitness function, function set, control parameters, terminal set, and termination criterion [30]. GEP process uses the principle of Darwin's evolution theory to optimize sets of symbols and variables to predict the relationship between the predictor and the predicted element. In the program, character strings at fixed length are adopted to represent the problem solutions, which are later presented as parse trees of various shapes and sizes known as GEP expression tree (ET). GEP is capable of producing model expression of the interactive process of the physical phenomenon's rules which other data-driven techniques like ANN, ANFIS, etc., do not exhibit [31], and it operates at the level of chromosome deployment that serve as expression trees (ET). Ferreira [32] has provided comprehensive information about all the genetic operators used in GEP, and Table 2 illustrates the specific approach and parameters used for conducting this study.

In order to use GeneXpro Tools 4.0, a dataset needs to be divided randomly into two subsets: the training and testing datasets. The training dataset is used to train the GEP using the genetic algorithm to minimize mean square error, while the testing dataset is used to evaluate the GEP's predictive performance. In this study, 75% of the data is used for training, and 25% is used for testing. The GEP's performance is measured using the correlation coefficient R and root mean square error RMSE [33].

Table 2 Summary of parameter settings used for the GEP simulation

Parameter	Setting
Number of chromosomes	30
Number of genes	3
Head size	8
Linking function	Addition
Function set	+, −, ×, ÷, x^2, sqrt
Constants per gene	2
Data type	Floating-point
Error type	RMSE with Parsimony Pressure
Constant bound (lower, upper)	−10, 10
Mutation rate	0.044
Inversion rate	0.1
IS transposition rate	0.1
RIS transposition rate	0.1
One-point recombination rate	0.3
Two-point recombination rate	0.3
Gene recombination rate	0.1
Gene transposition rate	0.1

2.4 Evaluating the impact of steel grouting on the embankment stability

Section 2.4 presents the impact of the steel grouting on the stability of the embankment and the numerical analysis conducted. The resistance of the steel pipe consolidation grouting method used in the Nanhu railway embankment under the impact of water level fluctuation is evaluated.

Generally, two kinds of connections are common for the Concrete filled steel-tube pipes grouting. These are reinforcement threaded and welding casing connections. In this study, Concrete filled steel-tubes (CSTs) were selected for their enhanced stiffness, compressive capacity, and ductility compared to concrete columns reinforcement. Stringent measures were taken to ensure that the connecting joints were free from all kinds of impurities. However, the usual CSTs are susceptible to corrosion of the outer surface. To mitigate corrosion, the CSTs were coated with anti-corrosive Epoxy Resin, providing protection against harsh environmental conditions. The CSTs used had two different sizes: ∅ 108 mm × 6 mm at 90° and ∅ 60 mm × 4 mm at 60°/30°. The CSTs connected with threaded ends were precisely placed at 1 m and 2 m equidistant row-wise into drilled holes, corresponding to their respective sizes and depths. The ∅ 108 mm × 6 mm CSTs were placed at a depth of 28 m, while the ∅ 60 mm × 4 mm CSTs were positioned at 15 m depth. The numerical analysis was conducted using the same CST specifications and arrangement as in the fieldwork, ensuring consistency between the two sets of data. Detailed information on the CST arrangement and specifications used in the study can be found in Fig. 1 (a), Fig. 5 and Table 3, providing an overview of the CST implementation for grouting reinforcement. In the numerical study, a sensitivity analysis of the angle of placement was conducted. Firstly, all CSTs grouting were placed vertically at 90°, and the safety factor was determined. In the second case, the tube with the smaller diameter was placed at 30°/60°, while the others remained at 90°. This analysis is presented to optimize the reinforcement strategy required to enhance slope stability, minimize risks of failure, and improve overall embankment performance. The placement of the steel pipe grouting, as illustrated in Fig. 1 (a), was determined based on the observed geotechnical behavior of the embankment and prior failure occurrences in the study area. Specifically, the grouting was introduced within the identified failure-prone zone, as shown in Fig. 1 (b), where differential hydraulic loading between the left and right lakes resulted in significant seepage forces and potential instability. It is important to note that the steel pipes themselves were not

Fig. 5 (a) Failure surface (b) Grouting process (c) Steel pipe (SP) materials

Table 3 Steel pipe reinforcement parameters

Label	Diameter (m)	Angle of placement (°)	Length (m)	Shear force (KN)	Thickness (m)
SP1a	0.06	30	15	1462	0.004
SP1b	0.06	60	15	1462	0.004
SP2	0.108	90	28	1462	0.006

modeled as discrete structural elements (e.g., beam elements); instead, their effect was incorporated through the improved material behavior of the surrounding grouted soil mass. This approach allows for a realistic and computationally efficient simulation of the reinforcement mechanism while capturing its influence on both seepage behavior and embankment stability.

3 Results

3.1 In situ site stress analysis

The result of the undrained shear strength analysis (as briefly discussed in Section "Deformation process and analysis") was obtained, and the range of values falls between 14–22 kPa, as shown in Fig. 6 (c). For clarity, the undrained shear strength values were determined in the ultimate state and account for the existing pore water pressure. This may be used to evaluate the stability of the Nanhu Railway embankment [34]. However, low undrained shear strength and the potential for negative and positive pore-water pressures (as shown in Fig. 6) may contribute to stability risk issues and make soil mass susceptible to deformation and failure under certain loading conditions, particularly at high pore-water pressure [35]. The result of the analysis further shows the deviatoric stresses of the embankment are more within the range from 0 to 400 kPa. Although some degree of variability in the stresses experienced by the embankment, suggests that it may be prone to failure under specific geological and environmental conditions. The changes in water levels on both sides create uneven stress distribution, leading to irregular cracking, unlike the water level on one side, which results in a more uniform rise in PWP [36].

3.2 Pore-water pressure conditions of the study area

The seepage fields of the Nanhu slope were simulated under water level scenarios, and the results were analyzed. The analysis revealed that the seepage at the embankment slope follows the typical seepage behavior and exhibits specific characteristics that align with earlier studies [37] as shown in Fig. 7. The seepage fields of the Nanhu slope were simulated under water level scenarios, and the results were analyzed. Further analysis reveals the pore-water pressure lines for both simulation scenarios. Scenario 1 shows an upward concave pattern, indicating that the slope's hysteresis becomes more obvious as the lake water level increases, that aligns with earlier studies [38], as shown in Fig. 7. As the lake water level declines, pore water pressure decreases, expanding the unsaturated area and decreasing saturation, which is in

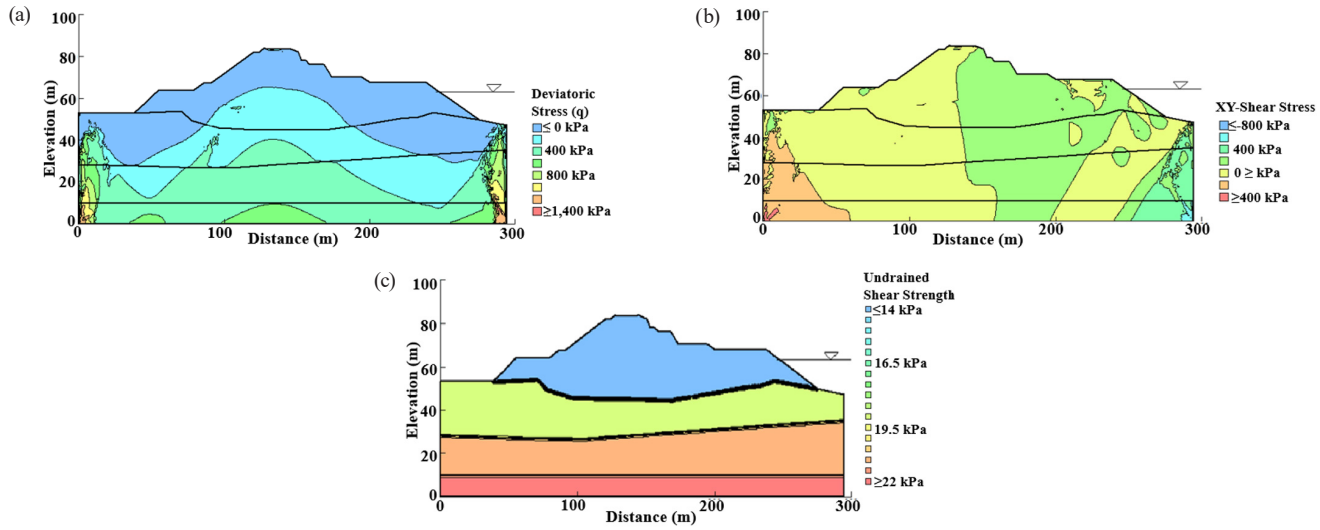

Fig. 6 In situ stresses conditions (a) Deviatoric stress, (b) XY-shear stress, and (c) Undrained shear strength

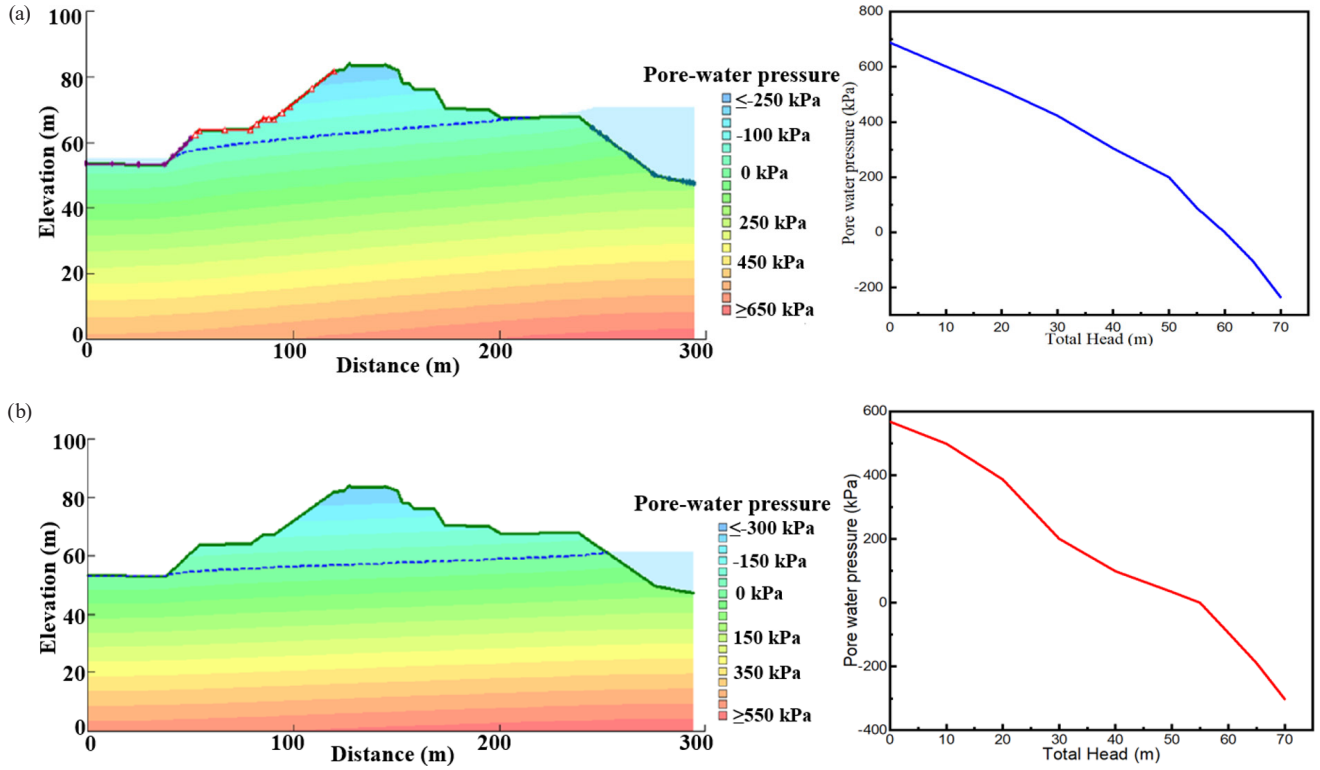

Fig. 7 Seepage and pore-water pressure vs. head profiles for (a) Scenario 1, (b) Scenario 2

agreement with the previous study [39]. Thus, the phreatic line flattens. This study found that the slope's phreatic line closely matches lake water level, affecting the seepage field. The pore-water pressure increases down the foundation due to the impact of the lake's water seepage. Negative pore-water pressure indicates that the soil is dry, and there is a suction force that draws water into the soil from surrounding areas. This can lead to soil shrinkage and reduced soil strength, which can have minor effects on the stability of the embankment [40]. As can be seen in Fig. 7, the pore-water pressure in scenarios 1 and 2 demonstrates changes in pore-water pressure from zero to 20 days period due to the abrupt rise in water level. Thus, the sudden rise in water level is detrimental to railway embankment, which previous studies are yet to capture.

Fig. 7 shows the relationship between pore-water pressure and total head. This aimed to present the correlation of pore-water pressure with changes in water level or drawdown based on the design scenarios. It is observed that scenario 1 is more sensitive. As the water level

increases, as shown in Fig. 7 (a), the pore-water pressure increases. For short water level fluctuations, as observed in scenario 2, the pore-water pressure remains steady within the embankment, but when a longer fluctuation is observed, the pore-water pressures vary significantly; on the premise of the Darcy theory, the phreatic surface line decline or rise simultaneously as water level changes. As the water level rises, the tendency for more water to seep into the slope increases, and this will lead to an increase in pore-water pressure and a decrease in soil suction (see Fig. 7). The phreatic line is basically controlled by the rate of change in soil suction, and these gradually impact the porosity and permeability [41], and they may induce cracks, which might result in embankment liquefaction and slope failure.

3.3 Deformation analysis

The relationship between pore-water pressure and total head for scenarios 1 and 2 was used to evaluate the deformation conditions of the embankment as depicted in Fig. 8. Having obtained the model result, to validate the accuracy of the finite element method (FEM) in GeoStudio 2D [17] software, an initial validation analysis was performed. So, the in situ deformation data of the embankment, which were collected during the period of five days in 2020, were compared to the two results that were found using FEM in PLAXIS 2D [16] and GeoStudio 2D [17] software when the water level changed. Note that the FEM models used have the same specifications and material properties based on the criteria used by previous study [34]. Fig. 8 shows the results from the PLAXIS 2D [16], GeoStudio 2D [17] models, and in situ measurements. It demonstrates a similar pattern, which indicates that the water infiltration into the embankment slope from the lake exhibits hydraulic hysteresis and manifests hydrostatic pressure changes. It is worth noting that the deformation observed through in situ monitoring (232 mm in the year 2020) and the simulation values in SIGMAW (232.69 mm at a drawdown rate of 0.2 m/d) are very similar in magnitude for scenario 2, while the deformation obtained in scenario 1 (238.43 mm at a drawdown rate of 0.1 m/d) and deformation for PLAXIS 2D [16] is 240 mm (see Fig. 8). The comparison reveals that the failure loads for the in situ measurements and the FEM models are similar, and the level of accuracy when compared with the observed is between 2% and 3% in the two models. Although the maximum error is only 3%, which is within the acceptable range [42]. This difference could be as result of the fact that the rise in water level has a fixed rate transient flow as considered in the numerical modelling. Also, the variation in hydraulic gradeline [36]. The fixed value used may not be a typical reflection of the real-time conditions [26], but due to the limitation of the model, the analysis is validated by the observed site data, Additionally, the existing complex natural environmental conditions may have a significant impact on real-time field conditions. Our observation suggests that faster drawdown has a greater negative impact on embankment stability, which is supported by a related study [3] conducted on the Xigouwan landslide using FLAC-3D model.

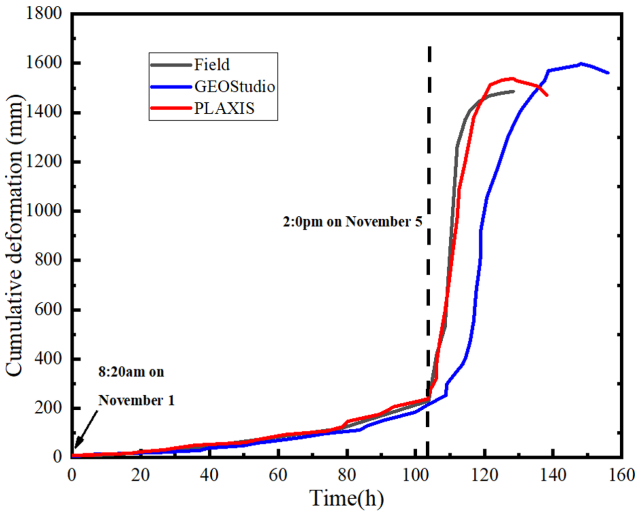

Fig. 8 Model validation results: relationship between deformation profiles of field measured, PLAXIS 2D [16] and GeoStudio 2D [17] models predictions for 5 days

In summary, from Fig. 8, prior to 8:20 AM on November 1st, the creep deformation of the railroad did not affect driving comfort. The first indication of train discomfort was reported by the train driver. Following this, precise monitoring was conducted every 2 hours using levelling tool to understand the deformation until the railroad's eventual collapse. As illustrated in Fig. 8, significant deformation commenced at 8:20 AM on November 1st and progressively worsened until the railroad slope fully collapsed Within 30 hours after 8:20 AM on November 1st, the deformation reached 35 mm, surpassing the cumulative deformation observed during the entire creep process in 2020. The deformation increased sharply to 232 mm by 2:00 PM on November 4th, 102 hours after the initial large deformation began. Due to excessive subsidence, the railroad was closed to traffic at this time. Ultimately, the cumulative subsidence exceeded 1200 mm within less than 20 hours, with the rate of deformation escalating abruptly.

3.4 Evaluation of Nanhu embankment stability

The stability analysis was conducted to examine the impact of the water levels of the two lakes considering the water drawdown on both sides of the lakes beside the failure plane of the Nanhu embankment stability that was analyzed. According to the previous studies, for steady-state conditions, the factor of safety (FOS) should be above 1.0 as a minimum [43], but FOS between 1.1–1.2 under rapid drawdown can be considered acceptable for earth fill [39]. Moreover, Nanhu embankment is considered stable for a factor of safety not less than 1.0, using various guidelines of railway embankment design [44, 45]. The embankment factor of safety obtained for drawdown scenario 2 (SC2) falls between 2.1256 to 0.9312; however, scenario 1 (SC1) shows a slightly different range from 2.116 to 0.9128 for an analysis period of 20 days, meaning that Nanhu embankment is relatively unstable. Fig. 9 illustrates the changes in the safety factor in response to the drawdown of the water in the lakes. It can be concluded that excess pore-water pressure can lead to a sudden decrease in the embankment's factor of safety [46]. It is important to note that the overall differences in the safety factor make it more evident that a sudden change in water level is a threat to the stability of an embankment. From Fig. 9 scenarios 1 and 2 demonstrate that changes in drawdown control the effective stress and shear strength of the soil [47]. Fig. 9 shows the variation in the factor of safety with time at different water levels. Authors further studies will provide the behavior law of the two water levels on either side of the railway embankment as a function of time.

3.5 Relationship between factor of safety, PWP, and static load

The FEM simulation results and the track loads were applied as input parameters (i.e., deformation, pore-water pressure) in developing the GEP models for Nanhu embankment during rising and falling water levels scenarios. The GEP analysis was successful in developing predictive models for the factor of safety, which is an essential parameter for assessing the stability of an embankment. Fig. 10 shows the correlation values (Adj. R^2) obtained from the regression analysis for the two scenarios are 0.67016 and 0.7926, respectively. These values indicate a strong correlation between the input variables (see Eqs. (2) and (3)) and the output variable in both scenarios [30]. The high values of R^2 suggest a good match between the input variables and the output variables, indicating that the suitability and precision of predictive models developed [33]. The root mean square error values (RMSE) obtained for the two scenarios are 0.0268 and 0.0087, respectively, as shown in Fig. 11. These values indicate the level of accuracy of the predictive models developed using GEP. The lower the value of RMSE, the higher the accuracy of the predictive model [33]. The RMSE values obtained in this study are relatively low, an indication that the predictive models developed using GEP are highly accurate as shown in Eqs. (2) and (3).

$$SF_f = \left(\left(\frac{P_w D_f}{L_s - 9.9977}\right) - D_f^{0.5} + D_f\right) + \left(\frac{P_w - 0.5L_s}{P_w - 2.1499L_s}\right) - \left(\frac{2.6957D_f - \left(D_f L_s\right)^{0.5}}{P_w^{0.5}}\right) \tag{2}$$

$$SF_r = \left(0.0551 + 2.0525D_f - D_f^{0.5}\right) - 3.1103\left(D_f - 1.8902D_f^2\right)^{0.5} + \frac{\left(2.0507\left(P_w D_f^{0.5} - L_s\right) - 1.7194\right)}{\left(P_w D_f^{0.5} + D_f - L_s\right)} \tag{3}$$

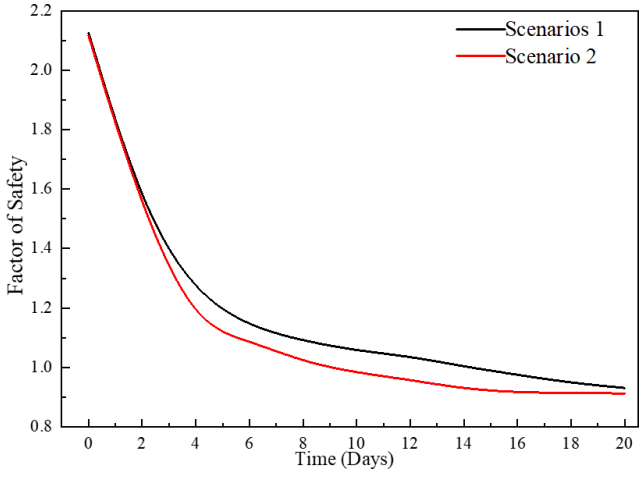

Fig. 9 Variation of the factor of safety with time at different water levels

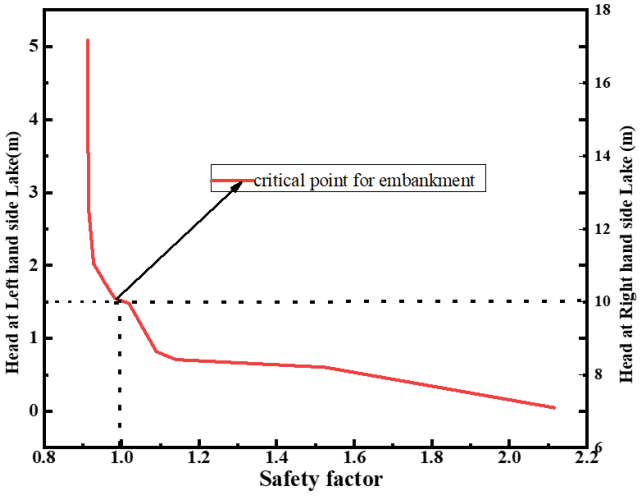

Fig. 10 Relationship between lakes water level and safety factor

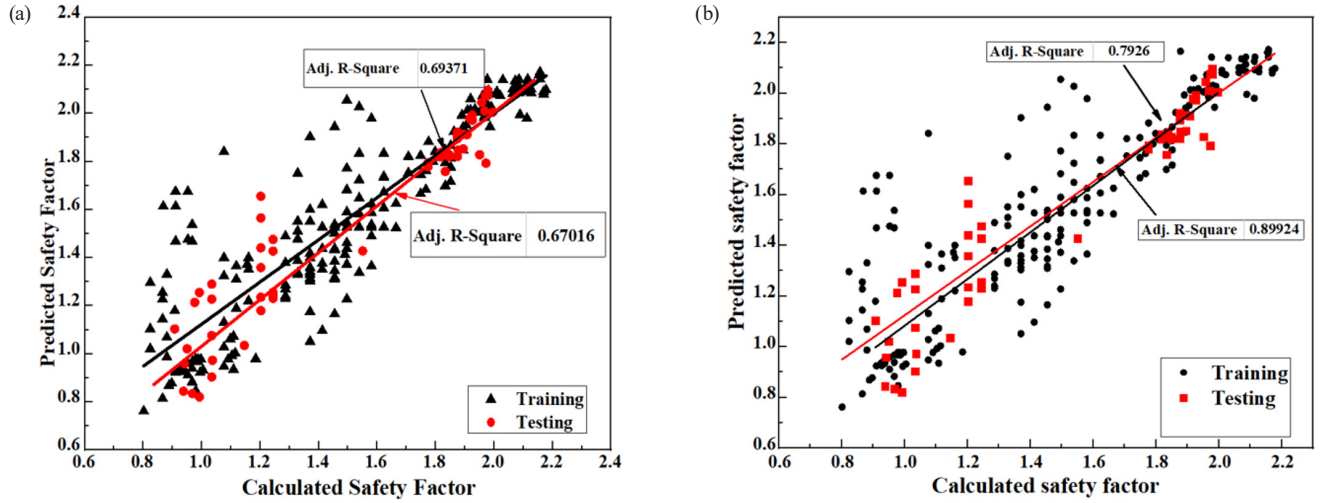

Fig. 11 Regression analysis of calculated versus predicted safety factors from GEP model for all data sets (a) Scenario 1 (b) Scenario 2

Where SF_f = safety factor at falling water level, SF_r = safety factor at rising water level, D_f = deformation, P_w = pore-water pressure, and L_s = static load.

3.6 Determination of Nanhu embankment stability water level thresholds

Fig. 10 presents the relationship between the water level on both sides of the railway embankment and the values of the factor of safety for static analysis. It indicates that at 9.9 m stage height from the right-hand side of the lake and 1.5 m on the left-hand side, the railway embankment stability value is around 1.0. which implies that above these water level thresholds, the railway embankment factor of safety will be below unity. The presence of water bodies on both sides of the embankment creates a higher hydraulic gradient, leading to an elevated PWP within the embankment. As the PWP fluctuates, it causes deformation and cracking in the weakened soil layers within this zone. This is evident in the agreement between the observed and numerical data depicted in Figs. 2 and 10.

3.7 Impact of steel grouting on embankment stability

The numerical analysis of a steel pipe grouted reinforced railway embankment was evaluated in terms of its stability strength, i.e., safety factor. As earlier emphasized, the embankment factor of safety should be greater than 1.0. Nanhu embankment, under the influence of water level variation, has a factor of safety ranging from 2.126 to 0.931 for the falling scenario and 2.116 to 0.9128 for the rising scenario, which implies that the embankment is not stable after 8 days for the rising scenario and 14 days for the falling scenario (as depicted in Fig. 9). When the embankment was reinforced using the steel pipe consolidation grouting method and placed at the potential failure surface (as shown in Fig. 12), it was observed that the safety factor of the reinforced embankment increased by 50% (see Fig. 12), i.e., the values increased from 1.415 to 3.231 for the falling scenario and 1.386 to 3.195 for the rising scenario, which shows that the embankment is stable throughout its critical period of 8 days and beyond. The results of the analysis have demonstrated similarity with results obtained in previous studies using various reinforcement materials [48]. Hence, steel pipe grouted reinforcement is reliable and feasible in mitigating embankment-related problems in dealing with the drawdown of water levels on both sides of an embankment.

4 Discussion of results

4.1 Embankment behavior under two faces water fluctuation conditions

During the monitoring process and studies in 2020, it was observed that the deformation actually began to show a trend on November 1, as the water level was receding, and on the 5th of the same month, when the water level was about 10 m (see Fig. 2). From the observed data, the slope slide, which agreed with the numerical analysis that revealed the slope becoming unstable at 1.5 m and 9.9 m during water level fluctuations as shown in Fig. 10. It shows that the slope may not necessarily slide at the highest water level, even when deformation shows its maximum. This is due to the equilibrium between the differential water pressure, geostatic pressure, and effective vertical stress [49]. Thus, water serves as a retaining structure for the slope surface. From Fig. 9, it is observed that the stability rapidly decreases in both scenarios and, after 10 days, depicts that the accumulated excess pore-water pressure no longer has

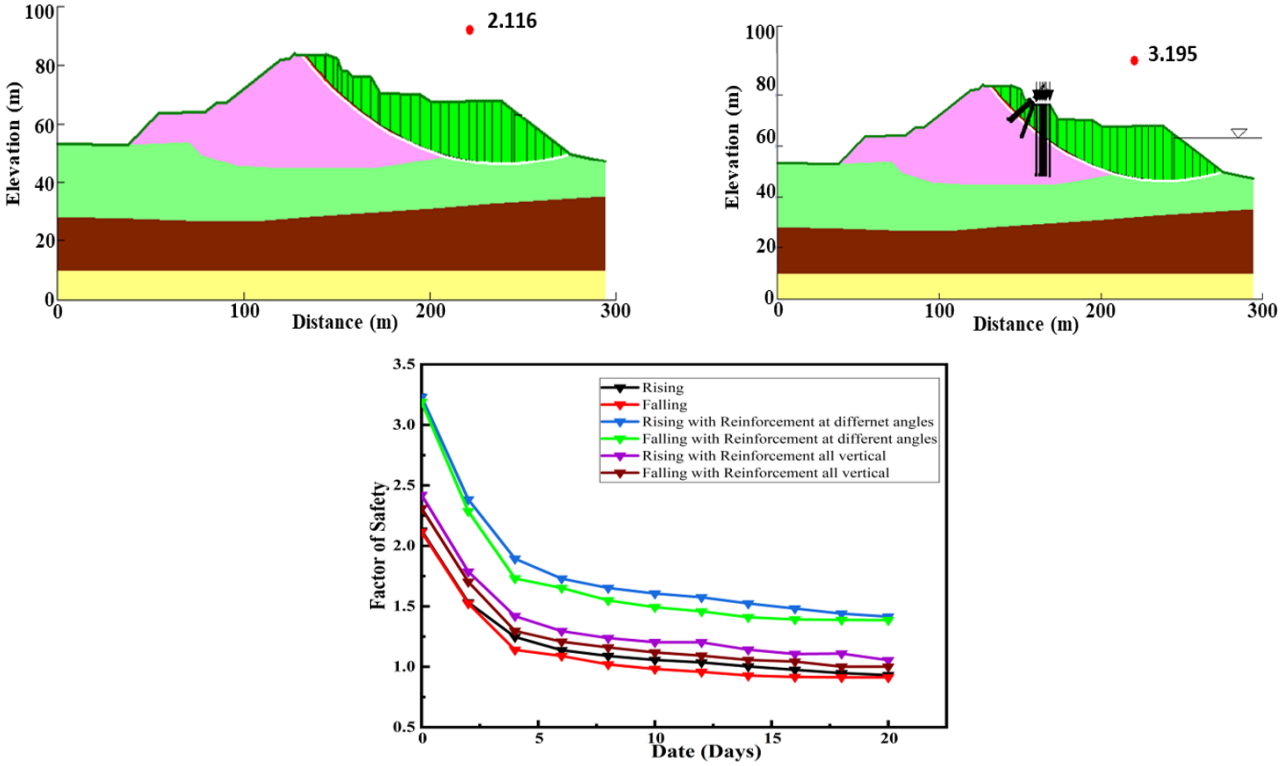

Fig. 12 Relationship between unreinforced and reinforced railway embankment FOS

a significant influence on the stability [50]. In this study, the observed deformation and numerical calculation are in good agreement, as shown in Fig. 8. The study shows that plastic deformation at the embankment toes is mainly caused by changes in water level, while at the crest, it is due to the combined impact of static train loads and lake water level fluctuations. Thus, the results of the investigations for strain analysis demonstrate that:

1. The settlement trend progressively develops from the internal structure to the surface mass, as noticed during the fieldwork as shown in Fig. 2. It was observed from the monitoring process in 2020 that the maximum water level of the lake is 71.2 m, which is detrimental to the slope stability because it weakens the soil mass even though the differential water pressure acts as a temporary retaining structure.
2. The drawdown scenario 2 revealed that during the period under consideration, a maximum cumulative deformation of 232.69 mm is observed from the numerical analysis, and the embankment exhibits slight fluctuations within a narrow range when the lakes water level rises, as a significant increase is recorded in deformation 238.43 mm (see Fig. 8). However, the embankment may not fail at that due to equilibrium between the geostatic force and the vertical stress.
3. Further analysis of the result shows that the deformation of the embankment is directly proportional to the pore water pressure, which does not contradict previous studies [46]. Indeed, the presence of water on both sides makes the embankment more susceptible to high infiltration, leading to a significant build-up of pore-water pressure. This, in turn, weakens the soil's shear strength and encourages internal erosion and particle migration, which ultimately results in differential settlement and deformation, compromising the embankment's stability.

4.2 Understanding the relation between safety factor, PWP, deformation, and static load for embankment stability management

Equations (2) and (3) demonstrate the relationship between PWP, strain deformation, train track loads, and the factor of safety for the two scenarios. The analysis reveals that as the matric suction dissipates due to an increase in PWP, plastic strain mobilizes at the slope surface, leading to the potential formation of cracks [49]. This cumulative strain deformation results in a reduction in the factor of safety (FOS), and when the FOS becomes less than 1.0, it indicates that embankment failure has occurred after this successive change in PWP.

Furthermore, the analysis indicates that with an increase in PWP, the track static load acts vertically on the slope, generating more vertical stress, which causes soil particle dissolution and migration due to saturation [51]. This process creates cracks and internal piping, thereby promoting slope instability. The primary cause of the embankment failure incident is the progressive rise and rapid drawdown of PWP, which generates unsteady groundwater, weakens the soil layer of the slope, and lack of sufficient drainage contributes to the sliding of the embankment slope. It can be inferred from the results depicted in Fig. 7 that the more the PWP, the more susceptible the embankment will be.

4.3 Impact of embankment reinforcement on the safety factor

After the failure incident in November 2020, the slope was reinforced with concrete columns, but another failure occurred shortly after. Subsequently, the idea of using CSTs grouting was introduced, and the slope was reinforced using this method. The grouting process filled the steel tubes with Concrete and was aimed at increasing the compressive capacity and stiffness of the embankment. CSTs grouting on the failure surface of an embankment increases the FOS by providing enhanced reinforcement, improved load distribution, increased bearing capacity, resistance to differential settlement [52], and resist risk slope failure. These multiple advantages are offered by CSTs grouting in terms of even distribution of load and stress. This balanced load distribution helps to prevent localized stress concentrations and reduces the risk of failure [53]. It can be inferred that CSTs grouting significantly increased the bearing capacity of the soil [52] compared to the earlier use of concrete columns. Furthermore, the study investigated the effects of the angle of placement of the CSTs and found that using a multi-angular system of 30°, 60°, and 90° was more efficient than placing all the CSTs vertically at 90°. The varying angles on the output of a numerical model help to understand the influence of uncertainties. In the context of placing steel pipes at different angles on the embankment, can provide valuable insights into the most effective and efficient angle arrangement, optimizing slope stability.

The multi-angular arrangement of CSTs interacted with the soil structure to create an anti-sliding bond, which effectively controlled the failure process and strengthened the failure area. The impact of the CSTs reinforcement on the slope stability, as measured by the FOS [1], can be observed in Fig. 12. The study introduces a new idea for reinforcement placement that is both feasible and reliable, and it can be applied in areas with complex hydrological and geological processes. However, the process of CSTs reinforcement can be further examined in terms of determining the optimal length for the reinforcement, which may provide additional insights for future applications.

5 Conclusions

The November 5, 2020 failure (Fig. 5 (a)) necessitated testing how a railway embankment reacts to increasing water levels on both sides, focusing on seepage, displacement, and stability. The study indicated that the Nanhu railway embankment's stability is affected by fluctuating lake water levels on both sides and track static load. These loads generate swift differential settlement, pore-water pressure changes, and factor of safety changes, with the maximum displacement recorded during increasing scenarios. The embankment is least safe with rising water levels, usually between April and October. The study also shows that a sudden decline rate, exceptionally high-water level, and track static loads negatively impact railway embankment stability. Thus, an early warning system for lake water levels is needed to direct railway operations during lake water level variations, which can damage the embankment. Also, the following are the key findings of this study: The stability factor of the Nanhu railway embankment drops from 2.116 to 0.9128 when the lake water level rises 0.1 m/day from 53.5 m to 71.2 m and 53.5 m to 58 m. In the second scenario, the water level drops at 0.2 m/day and the embankment stability factor drops from 2.1256 to 0.9312. The stress state to be considered when designing this type of railway embankment is the scenario of rapid lowering of water levels because the stability is weakest at this stage. The numerical analysis shows that fast water level changes and prolonged immersion influence the railway embankment's stability. This caused significant deformations of 232.69 mm, 238.43 mm (SIGMAW), and 240 mm (PLAXIS 2D [16]), notably at high water levels and vehicle loads. Observations from monitoring points across the failed surface revealed inconsistent displacement curves, indicating partial deformation. Notably, the K1430 + 110 failed surface displayed a step-like displacement pattern, attributed to repeated fluctuations in lakes levels. Analysis of displacement time curves suggested a seasonal cycle closely linked to hydrological factors like lake levels and rainfall. The slope movements exhibited rapid displacement over short periods, succeeded by prolonged low strain rates. As shown

in Fig. 9, the safety factors indicate unstable embankment conditions for 8 days in both scenarios with FOS < 1.0. Thus, the thresholds for lake water levels on both sides for Nanhu railway embankment stability were 1.5 m and 9.9 m, which will serve as early warning parameters for system design. However, other environmental variables may affect railway embankment susceptibility.

The study also reveals that the Concrete filled steel-pipe grouting consolidation method can improve the stability of the railway embankment by 50% under the influence of water level changes on both sides of the slope as shown in Fig. 12. Also, GEP was employed to predict the factor of safety using pore-water pressure, train static loads, and deformation (see Eqs. (2) and (3)). GEP models are suitable to evaluate embankment stability through safety factors.

Declaration of competing interest

The authors declare that the paper has no financial interests and personal relationships that have could influence the study report.

Acknowledgments

This work was supported by the National Natural Science Foundation of China (U2268213), the China Railway Group Limited Technology Research and Development Plan (2023-key Project-09), and the China Railway Group Limited Technology Research and Development Plan (2022-Special-07-High-Speed Railway).

Data availability

Data will be made available on request.

References

[1] Lazorenko, G., Kasprzhitskii, A., Kukharskii, A., Kochur, A., Yavna, V. "Failure analysis of widened railway embankment with different reinforcing measures under heavy axle loads: A comparative FEM study", Transportation Engineering, 2, 100028, 2020. https://doi.org/10.1016/j.treng.2020.100028

[2] Linrong, X., Usman, A. B., Bello, A.-A. D., Yongwei, L. "Rainfall-induced transportation embankment failure: A review", Open Geosciences, 15(1), 20220558, 2023. https://doi.org/10.1515/geo-2022-0558

[3] Zhang, Y., Zhu, S., Tan, J., Li, L., Yin, X. "The influence of water level fluctuation on the stability of landslide in the Three Gorges Reservoir", Arabian Journal of Geosciences, 13(17), 845, 2020. https://doi.org/10.1007/s12517-020-05828-3

[4] Liu, K., Wang, M., Cao, Y., Zhu, W., Yang, G. "Susceptibility of existing and planned Chinese railway system subjected to rainfall-induced multi-hazards", Transportation Research Part A: Policy and Practice, 117, pp. 214–226, 2018. https://doi.org/10.1016/j.tra.2018.08.030

[5] Moretti, L., Loprencipe, G. "Climate change and transport infrastructures: State of the art", Sustainability, 10(11), 4098, 2018. https://doi.org/10.3390/su10114098

[6] Niu, F., Hu, H., Liu, M., Ma, Q., Su, W. "Studies for frost heave characteristics and the prevention of the high-speed railway roadbed in the Zoige Wetland, China", Frontiers in Earth Science, 9, 678655, 2021. https://doi.org/10.3389/feart.2021.678655

[7] Aqib, M., Usmani, S., Khan, T., Sadique, M. R., Alam, M. M. "Experimental and numerical analysis of rainfall-induced slope failure of railway embankment of semi high-speed trains", Journal of Engineering and Applied Science, 70(1), 20, 2023. https://doi.org/10.1186/s44147-023-00188-7

[8] Roshan, M. J., Rashid, A. S. A., Wahab, N. A., Hezmi, M. A., Jusoh, S. N., Azmi, M. "Stability of railway embankment in saturated and unsaturated conditions", IOP Conference Series: Materials Science and Engineering, 1153(1), 012007, 2021. https://doi.org/10.1088/1757-899X/1153/1/012007

[9] Kite, D., Siino, G., Audley, M. "Detecting Embankment Instability Using Measurable Track Geometry Data", Infrastructures, 5(3), 29, 2020. https://doi.org/10.3390/infrastructures5030029

[10] Burman, A., Singh, V. K., Kumar, V., Himanshu, N., Maity, D. "Seepage Analysis of Railway Earthen Embankment in Mokama Using RFEM Considering Random Hydraulic Conductivity Field", Geotechnical and Geological Engineering, 38(5), 5097, 2020. https://doi.org/10.1007/s10706-020-01350-1

[11] Liu, S. Y., Shao, L. T., Li, H. J. "Slope stability analysis using the limit equilibrium method and two finite element methods", Computers and Geotechnics, 63, pp. 291–298, 2015. https://doi.org/10.1016/j.compgeo.2014.10.008

[12] Zhao, L., You, G. "Rainfall affected stability analysis of Maddingley Brown Coal eastern batter using Plaxis 3D", Arabian Journal of Geosciences, 13(20), 1071, 2020. https://doi.org/10.1007/s12517-020-06038-7

[13] Gu, X., Ou, Q., Zhang, W., Fu, J., Hao, S. "A novel subroutine for estimating unsaturated slope stability considering water fluctuation in spatially variable soils", Bulletin of Engineering Geology and the Environment, 82(1), 6, 2023. https://doi.org/10.1007/s10064-022-03025-y

[14] Gupta, R. K., Chawla, S. "Performance evaluation of micropiles as a ground improvement technique for existing railway tracks: Finite-element and genetic programming approach", International Journal of Geomechanics, 22(3), 04021287, 2022. https://doi.org/10.1061/(ASCE)GM.1943-5622.0002270

[15] Wang, L., Wu, C., Gu, X., Liu, H., Mei, G., Zhang, W. "Probabilistic stability analysis of earth dam slope under transient seepage using multivariate adaptive regression splines", Bulletin of Engineering Geology and the Environment, 79(6), pp. 2763–2775, 2020. https://doi.org/10.1007/s10064-020-01730-0

[16] Bentley "PLAXIS 2D, (Version 2022)", [computer program] Available at: https://www.bentley.com/software/plaxis-2d/

[17] Seequent "GeoStudio 2D, (Version 2012)", [computer program] Available at: https://www.seequent.com/products-solutions/geostudio-2d/

[18] Krahn, J. "Limit equilibrium, strength summation and strength reduction methods for assessing slope stability", In: Rock Mechanics: Meeting Society's Challenges and Demands, Vancouver, Canada, 2007, pp. 311–318. ISBN 978-0-415-44401-9

[19] Wang, J., Xu, Y., Zhang, D., Gu, T. "Vibration-induced acceleration of infiltration in loess", Science China Earth Sciences, 64(4), pp. 611–630, 2021. https://doi.org/10.1007/s11430-020-9741-x

[20] Li, S., Li, Y., Xu, L. "Deformation Pattern and Failure Mechanism of Railway Embankment Caused by Lake Water Fluctuation Using Earth Observation and On-Site Monitoring Techniques", Water, 15(24), 4284, 2023. https://doi.org/10.3390/w15244284

[21] Sun, X., Du, Y., Deng, Y., Fan, H., Ma, T., Gan, Y. "Contrasting nutrients input along with groundwater discharge to east Dongting Lake, central China: A geological perspective", Ecological Indicators, 145, 109658, 2022. https://doi.org/10.1016/j.ecolind.2022.109658

[22] Wei, R., Tang, S., Ouyang, Q., Lu, T., Hu, B. X. "Study on the groundwater system of the Dongting Lake Plain, central-south China: a tectonic perspective", Hydrogeology Journal, 30(2), pp. 707–721, 2022. https://doi.org/10.1007/s10040-021-02436-7

[23] Autodesk "AutoCAD, (Version 2018)", [computer program] Available at: https://www.autodesk.com/eu/products/autocad/overview

[24] Dai, Z., Guo, J., Yu, F., Zhou, Z., Li, J., Chen, S. "Long-term uplift of high-speed railway subgrade caused by swelling effect of red-bed mudstone: case study in Southwest China", Bulletin of Engineering Geology and the Environment, 80(6), pp. 4855–4869, 2021. https://doi.org/10.1007/s10064-021-02220-7

[25] Aliyu, B. U., Xu, L., Bello, A.-A. D., Shuaibu, A., Kalin, R. M., Ahmad, A., Islam, N., Raza, B. "Prediction of Railway Embankment Slope Hydromechanical Properties under Bidirectional Water Level Fluctuations", Applied Sciences, 14(8), 3402, 2024. https://doi.org/10.3390/app14083402

[26] Shoaib, M., Yang, W., Liang, Y., Rehman, G. "Stability and deformation analysis of landslide under coupling effect of rainfall and reservoir drawdown", Civil Engineering Journal, 7(7), pp. 1098–1111, 2021. https://doi.org/10.28991/cej-2021-03091713

[27] Kim, S. W., Chun, K. W., Kim, M., Catani, F., Choi, B., Seo, J. I. "Effect of antecedent rainfall conditions and their variations on shallow landslide-triggering rainfall thresholds in South Korea", Landslides, 18(2), pp. 569–582, 2021. https://doi.org/10.1007/s10346-020-01505-4

[28] Mohsan, M., Vardon, P. J., Vossepoel, F. C. "On the use of different constitutive models in data assimilation for slope stability", Computers and Geotechnics, 138, 104332, 2021. https://doi.org/10.1016/j.compgeo.2021.104332

[29] Gandomi, A. H., Roke, D. A. "Assessment of artificial neural network and genetic programming as predictive tools", Advances in Engineering Software, 88, pp. 63–72, 2015. https://doi.org/10.1016/j.advengsoft.2015.05.007

[30] Jalal, F. E., Iqbal, M., Ali Khan, M., Salami, B. A., Ullah, S., Khan, H., Nabil, M. "Indirect Estimation of Swelling Pressure of Expansive Soil: GEP versus MEP Modelling", Advances in Materials Science and Engineering, 2023, 1827117, 2023. https://doi.org/10.1155/2023/1827117

[31] Kisi, O., Shiri, J., Nikoofar, B. "Forecasting daily lake levels using artificial intelligence approaches", Computers & Geosciences, 41, pp. 169–180, 2012. https://doi.org/10.1016/j.cageo.2011.08.027

[32] Ferreira, C. "What is gep?", GeneXproTools Tutorials – A Gepsoft Web Resource, 2007. [online] Available at: https://www.gepsoft.com/tutorial002.htm

[33] Meng, J., Mattsson, H., Laue, J. "Three-dimensional slope stability predictions using artificial neural networks", International Journal for Numerical and Analytical Methods in Geomechanics, 45(13), pp. 1988–2000, 2021. https://doi.org/10.1002/nag.3252

[34] Kassou, F., Bouziyane, J. B., Ghafiri, A., Sabihi, A. "Slope stability of embankments on soft soil improved with vertical drains", Civil Engineering Journal, 6(1), pp. 164–173, 2020. https://doi.org/10.28991/cej-2020-03091461

[35] Dai, G., Zhang, F., Wang, Y. "Stability analysis of layered slopes in unsaturated soils", Frontiers of Structural and Civil Engineering, 16(3), pp. 378–387, 2022. https://doi.org/10.1007/s11709-022-0808-2

[36] Sun, Y., Li, Z., Yang, K., Wang, G., Hu, R. "Analysis of the influence of water level change on the seepage field and stability of a slope based on a numerical simulation method", Water, 15(2), 216, 2023. https://doi.org/10.3390/w15020216

[37] Yan, Z.-L., Wang, J.-J., Chai, H.-J. "Influence of water level fluctuation on phreatic line in silty soil model slope", Engineering Geology, 113(1–4), pp. 90–98, 2010. https://doi.org/10.1016/j.enggeo.2010.02.004

[38] Showkat, R., Mohammadi, H., Babu, G. L. S. "Effect of rainfall infiltration on the stability of compacted embankments", International Journal of Geomechanics, 22(7), 04022104, 2022. https://doi.org/10.1061/(ASCE)GM.1943-5622.0002425

[39] Siacara, A. T., Beck, A. T., Futai, M. M. "Reliability analysis of rapid drawdown of an earth dam using direct coupling", Computers and Geotechnics, 118, 103336, 2020. https://doi.org/10.1016/j.compgeo.2019.103336

[40] Guo, C., Zhang, Y., Yuan, H., Liu, D., Yan, Y., Hua, S., Ren, S. "Study of an ancient landslide reactivation mechanism based on centrifuge model testing: an example of the Jiangdingya ancient landslide reactivation in 2018, Gansu Province, China", Landslides, 20(1), pp. 127–141, 2023. https://doi.org/10.1007/s10346-022-01978-5

[41] Jia, Y., Ding, Y., Wang, X., Zhang, J., Chen, X. "A Numerical Analysis of the Leakage Characteristics of an Embankment Dam Slope With Internal Erosion", Frontiers in Earth Science, 10, 953, 2022. https://doi.org/10.3389/feart.2022.866238

[42] Dyson, A. P., Tolooiyan, A. "Probabilistic investigation of RFEM topologies for slope stability analysis", Computers and Geotechnics, 114, 103129, 2019. https://doi.org/10.1016/j.compgeo.2019.103129

[43] Vrubel, J., Říha, J. "Discussion on the safety factors of slopes recommended for small dams", Acta Universitatis Agriculturae et Silviculturae Mendelianae Brunensis, 65(2), pp. 569–576, 2017. https://doi.org/10.11118/actaun201765020569

[44] UIC "UIC Code 719 R Earthworks and Track-bed Layers for Railway Lines", International Union of Railways, Paris, France, 1994.

[45] US Army Corps of Engineers "Engineering and Design: Slope Stability", [pdf] US Army Corps of Engineers, Washington, DC, USA, Rep. EM 1110-2-1902, 2003. Available at: https://www.publications.usace.army.mil/Portals/76/Publications/EngineerManuals/EM_1110-2-1902.pdf

[46] Yu, S., Ren, X., Zhang, J., Wang, H., Wang, J., Zhu, W. "Seepage, deformation, and stability analysis of sandy and clay slopes with different permeability anisotropy characteristics affected by reservoir water level fluctuations", Water, 12(1), 201, 2020. https://doi.org/10.3390/w12010201

[47] Mu, Y., Ma, W., Li, G., Mao, Y., Liu, Y. "Long-term thermal and settlement characteristics of air convection embankments with and without adjacent surface water ponding in permafrost regions", Engineering Geology, 266, 105464, 2020. https://doi.org/10.1016/j.enggeo.2019.105464

[48] Divya Jyothi, B., Ramya Krishna, V. "Optimal arrangement of geogrids in road embankment using different fill materials", Materials Today: Proceedings, 46, pp. 8507–8512, 2021. https://doi.org/10.1016/j.matpr.2021.03.510

[49] Dai, G., Gao, Y., Zhang, F., Shu, S. "Stability of layered soil slope with tension crack: A closed-form solution", Canadian Geotechnical Journal, 61(2), pp. 328–343, 2024. https://doi.org/10.1139/cgj-2022-0566

[50] Kafle, L., Xu, W.-J., Zeng, S.-Y., Nagel, T. "A numerical investigation of slope stability influenced by the combined effects of reservoir water level fluctuations and precipitation: A case study of the Bianjiazhai landslide in China", Engineering Geology, 297, 106508, 2022. https://doi.org/10.1016/j.enggeo.2021.106508

[51] Chen, M.-l., Qi, S.-c., Lv, P.-f., Yang, X.-g., Zhou, J.-w. "Hydraulic response and stability of a reservoir slope with landslide potential under the combined effect of rainfall and water level fluctuation", Environmental Earth Sciences, 80(1), 25, 2021. https://doi.org/10.1007/s12665-020-09279-7

[52] Huang, H., Jia, B., Lian, J., Wang, W.-W. "Experimental investigation on the tensile performance of resin-filled steel pipe splices of BFRP bars", Construction and Building Materials, 242, 118018, 2020. https://doi.org/10.1016/j.conbuildmat.2020.118018

[53] Chen, H., Wu, L., Jiang, H., Liu, Y. "Seismic performance of prefabricated middle frame composed of special-shaped columns with built-in lattice concrete-filled circular steel pipes", Structures, 34, pp. 1443–1457, 2021. https://doi.org/10.1016/j.istruc.2021.08.062